Ultrafast Degenerate Four Wave Mixing Studies of Third-Order Nonlinearities in Conjugated Organic Polymers Containing Azo Groups and Alkynyl Linkages in the Polymer Backbone

Darius Kuciauskas,*,† Michael J. Porsch,† Saulius Pakalnis,† Kimberly M. Lott,† and Michael E. Wright*,‡

Department of Chemistry, Virginia Commonwealth University, Richmond, Virginia 23284-2006 and Chemistry & Materials Division, NAWCWD, Code 4T4220D, China Lake, California 93555

Received: September 4, 2002; In Final Form: December 9, 2002

The first series of conjugated organic polymers with the formula {1,4-[2-(RO)-5-(R′O)C_6H_2]—N═N—C_6H_4—C≡C−}$_n$, where R = methyl, R′ = hexyl (**7a**) and R = hexyl, R′ = $SiMe_2$-*t*-Bu (**8**), were produced in palladium-catalyzed cross-coupling and homocoupling reactions of selected bis(bromo) and bis(alkynyl) azo monomers. The molecular weights (M_n) for the conjugated polymers ranged from 5500 to 22 000. Degenerate four wave mixing (DFWM) with 780 nm femtosecond pulses was used to investigate electronic third-order nonlinearities for azo monomer **3a** and conjugated azo polymer **7a**. Both compounds had ultrafast nonlinearities with $\tau_1 = 100$ fs response time. The real part of **7a** second hyperpolarizability, γ_{7a}, is negative, Re $\gamma_{7a} = -(4.3 \pm 0.3) \times 10^{-46}$ m^5 V^{-2}. Polymer **7a**'s second hyperpolarizability also has an imaginary component, Im $\gamma_{7a} = (1.7 \pm 0.3) \times 10^{-46}$ m^5 V^{-2}. Calculated per repeat unit, polymer $|\gamma_{7a}| = (4.6 \pm 0.5) \times 10^{-46}$ m^5 V^{-2} and is about 780 times larger than that for monomer **3a**. γ_{7a} was analyzed with the three-level model; γ_{7a} enhancement is attributed to the conjugation effects in the polymer and contributions from a two-photon state. Polymer **7a**'s excited state had a 3.4 ps lifetime, as determined by DFWM.

Introduction

Conjugated organic polymers possess a unique combination of electronic and optical properties. In recent years variations in structure have produced conjugated polymers with excellent solubility, adequate thermal stability, and intriguing optical properties.[1] It is the ability to tailor and make systematic structural changes at the molecular level that has made possible the concept of "molecular electronics".[2]

Although many types of linkages have been placed in the backbone of conjugated polymers, including such examples as heterocycles, vinyl, ethynyl, and various hydrocarbon aromatic rings, we are not aware of any conjugated polymer containing the azo linkage. Polymers containing the azo linkage[3] have a rich history of use in imaging (e.g., holographic storage) and more recently azo-containing polymers have shown the ability to generate surface relief gratings by simple irradiation.[4−6] It was recently suggested that azo dyes and polymers are potentially useful in optical switching applications between 600 and 900 nm and 1100−1500 nm.[7]

In this paper we report the synthesis and nonlinear optical studies of the first conjugated organic polymers to contain the azo linkage in the polymer backbone:

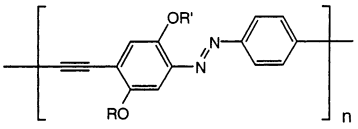

Conjugated Azo Polymers

DFWM results show that the second hyperpolarizability of this polymer is much higher than that for nonconjugated azo dyes, making materials incorporating azo functional groups and rigid alkynyl linkages interesting for further studies and nonlinear optical device applications.

Experimental Section

Methods. All manipulations of compounds and solvents were carried out by using standard Schlenk techniques. Solvents were degassed and purified by distillation under nitrogen from standard drying agents. Infrared spectra were measured with a Perkin-Elmer 1750 FT-IR spectrometer; UV−vis spectra, with HP-8452A and Ocean Optics USB2000. ^{1}H NMR and ^{13}C NMR measurements were performed using Bruker AC-200 MHz, Varian Mercury 300 MHz, or Varian Inova 400 MHz spectrometers. ^{1}H NMR and ^{13}C NMR chemical shifts are reported versus the respective solvent residue peak (solvent, ^{1}H, ^{13}C: $CDCl_3$, δ 7.25 ppm, δ 76.9 ppm; DMSO-d_6, δ 2.62 ppm, δ 36.9 ppm). The organic reagents were purchased from Aldrich Chemical Co. and used as received. Size exclusion chromatography (SEC) data were collected on a Hewlett-Packard 1100 HPLC system employing a PL size-exclusion column (300 × 7.5 mm, 5 μm particle size). Molecular weight data are referenced relative to polystyrene standards. Polymer analyses were preformed using a Perkin-Elmer TGA 7 and DSC 7 system. Elemental analyses were performed at Atlantic Microlab Inc., Norcross, GA.

Experimental Setup for Femtosecond Nonlinear Spectroscopy. The regeneratively amplified femtosecond Ti:sapphire laser system (Spectra Physics) produces 1 mJ pulses at 1 kHz repetition rate. The laser wavelength was set at 780 nm. The autocorrelation function of the instrument was monitored by measuring noncollinear second harmonics generation in a 0.5

† Virginia Commonwealth University.
‡ NAWCWD.

10.1021/jp026908o CCC: $25.00
Published on Web 01/28/2003

SCHEME 1: DFWM Experimental Setup[a]

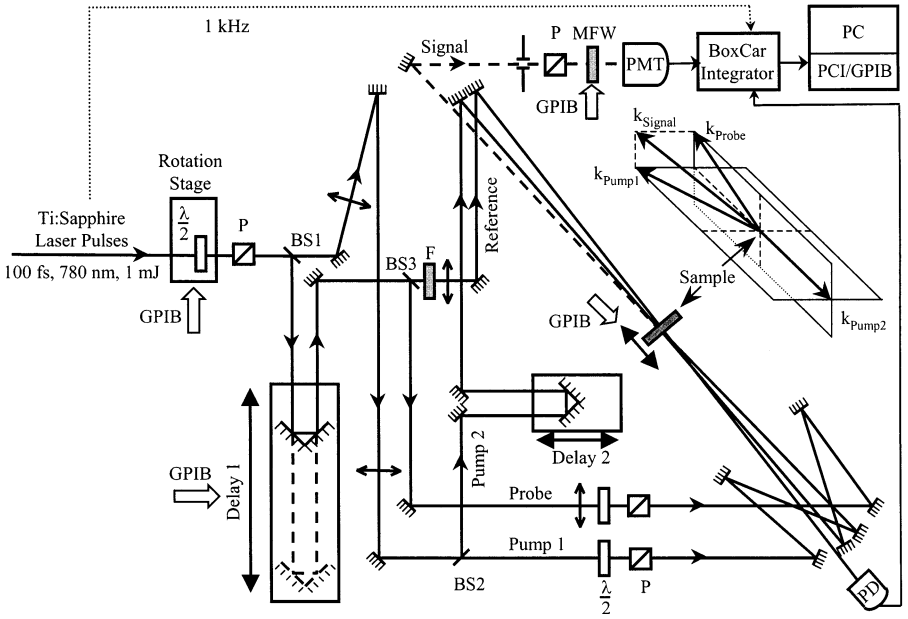

[a] Key: $\lambda/2$, zero-order waveplates; P, Glan laser polarizers; BS1, BS2, BS3, beamsplitters; PD, photodiode; PMT, photomultiplier; MFM, motorized filter wheel; F, OD = 4 neutral density filter; PC, personal computer; PCI/GPIB, computer control interface. Inset: four wave mixing signal $\vec{k}_{signal}$ is observed at the phase-matched direction so that $\vec{k}_{pump1} + \vec{k}_{pump2} + \vec{k}_{probe} + \vec{k}_{signal} = 0$, where $\vec{k}_i$ are wavevectors of the four beams.

TABLE 1: Maximal Pulse Energies and Intensities Used in DFWM Experiments

beam	pulse energy, μJ	beam radius,[a] mm	peak intensity,[b] G W cm^{-2}
pump 1	84	1.0	19.5
pump 2	72	1.0	16.3
probe	50	1.2	8.4

[a] The beam radius is taken as the radial distance at which the intensity fell to half of its value, assuming a cylindrical TEM_{00} mode intensity distribution. [b] Average peak intensity is calculated as (pulse energy) $\times$ $(\tau_p)^{-1}$ $\times$ $(\pi \times \text{radius}^2)^{-1}$ assuming $\tau_p = 130$ fs.

mm BBO crystal. The typical autocorrelation function had a full-width at half-maximum (FMHM) of 150−200 fs.

The degenerate four wave mixing (DFWM) setup utilizes near-counter propagating beam geometry (Scheme 1).[8,9]

Three beam splitters (BS1, BS2, and BS3) separate probe, pump, and reference pulses. Pump and probe pulses overlap in the sample as shown in the Inset of Scheme 1. Pump beams are collimated to a 1.0 mm radius with two planar-convex lenses. The probe beam is focused with a $f = 1500$ mm planar-convex lens; the probe beam radius at the sample holder is 1.2 mm. Time dependence of nonlinear signals was measured by delaying probe pulse with the computer-controlled translation stage (ILS250, Newport). A computer-controlled rotation stage (SR50, Newport) with a zero-order $\lambda/2$ waveplate and a Glan laser polarizer was used to control excitation intensity. The highest pulse energies and intensities used in the measurements are summarized in Table 1.

Reproducible sample positioning was achieved by translating the sample cell with the 1 in. stage and the computer-controlled motorized actuator (CMA-12CCCL, Newport) to maximize the nonlinear signal (Scheme 1). The thickness of the transient grating formed by the pump pulses in the sample was also measured by translating the sample. When the angle between the pump 1 and pump 2 beams was 174° and the angle between pump 1 and probe beams was 6°, the fwhm of the transient grating was ~60 μm.

To monitor laser pulse energy and sample stability, an additional reference beam was aligned through the sample and measured with an amplified photodiode. The reference beam was attenuated with a neutral OD = 4 filter and passed through the sample about 3 ns before the pump pulses.

The DFWM signal is spatially separated from the pump and the probe and is propagating in the direction satisfying the phase-matching conditions (inset in Scheme 1). The DFWM signal was detected with the near-IR sensitive photomultiplier (H6780-20 photosensor module with R7400U-20 PMT tube, Hamamatsu). A computer-controlled motorized filter wheel was placed in front of the photodetector and allowed measurements in a wide dynamic optical signal range. The PMT signal was amplified with the 300 MHz preamplifier (SR445, Stanford Research Systems). Photomultiplier and photodiode signals were gated and integrated with the boxcar signal averagers (SR255, Stanford Research Systems) and digitized by the 16 bit ADC card (PCI-6035E, National Instruments) in the personal computer. Lab View based software was developed to collect the signal and reference data and to control the delay line, the rotation stage, the sample positioning stage, and the motorized filter wheel. Several thousand data points were collected and averaged for each measurement (at a rate of 1000 data points per second). Only the data points for which reference pulse energy differed from the average by less than two standard deviations were included in the analysis.

For DFWM experiments, samples were dissolved in freshly distilled THF, filtered through a 0.45 μm PTFE syringe filter, and placed in 1 mm path length quartz cells. Solutions were magnetically stirred during experiments by placing a small stirring bar (Aldrich) in the sample cell (to fit into the 1 mm path length cell, the Teflon coating of the stirring bar was removed). Sample stability was checked by UV−vis absorption.

Degenerate Four Wave Mixing (DFWM). Third-order nonlinear polarization, $P_i^{(3)}$, as measured by DFWM, is given by[10]

$$P_i^{(3)} = \frac{3}{2}\epsilon_0 \chi_{ijkl}^{(3)} E_j E_k E_l \qquad (1)$$

SCHEME 2

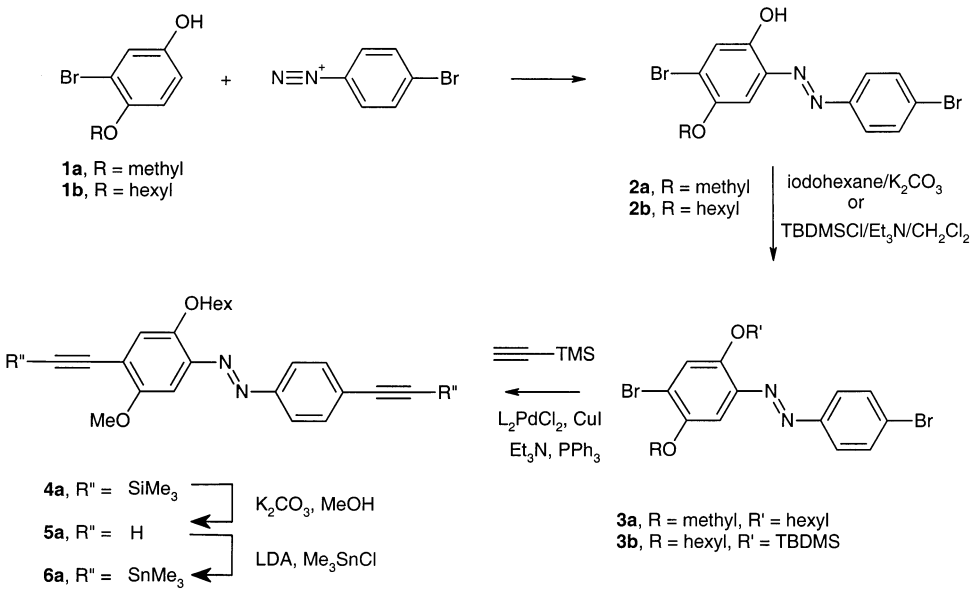

where ϵ_0 is a dielectric constant, E_j, E_k, E_l are amplitudes of electric field components, and $\chi^{(3)}_{ijkl}$ is a third-order nonlinear susceptibility tensor. In DFWM, both real and imaginary parts of $\chi^{(3)}_{ijkl}$ contribute to the signal, I_{sample}, and the signal is given by[11]

$$I_{\text{sample}} = (\chi^{(3)}_{\text{sample}})^2 \frac{l_{\text{sample}}^2}{n_{\text{sample}}^4}\left(\frac{1-\exp(-\alpha l_{\text{sample}})}{\alpha l_{\text{sample}}}\right)^2 \times \exp(-\alpha l_{\text{sample}}) I_{\text{pump1}} I_{\text{pump2}} I_{probe} \quad (2)$$

where l_{sample} is the optical pathlength, n_{sample} is the refractive index, and I_{pump1}, I_{pump2}, I_{probe} are intensities of respective beams. The absorption coefficient, α, includes both linear (α_0) and nonlinear absorption: $\alpha = \alpha_0 + \alpha_2 I + ...$, where α_2 is a two-photon absorption coefficient and I is intensity (when all three beams overlap in the sample cell, $I = I_{\text{pump1}} + I_{\text{pump2}} + I_{\text{probe}}$). Solution third-order susceptibility is determined from comparison with the known reference, usually solvent:

$$\chi^{(3)}_{\text{sample}} = \chi^{(3)}_{\text{solvent}} \sqrt{\frac{I_{\text{sample}}}{I_{\text{solvent}}}}\left(\frac{n_{\text{solvent}}}{n_{\text{sample}}}\right)^2 \frac{l_{\text{sample}}}{l_{\text{solvent}}} \times \left(\frac{\alpha l_{\text{sample}}}{1-\exp(-\alpha l_{\text{sample}})}\right)\exp\left(\frac{\alpha l_{\text{sample}}}{2}\right) \quad (3)$$

(it is assumed that the solvent does not absorb at the experiment wavelength). At low sample concentrations $n_{\text{sample}} \approx n_{\text{solvent}}$ ($n_{\text{solvent}} = 1.407$ for THF),[12] and $l_{\text{sample}} = l_{\text{solvent}}$ when the experiment is carried out in identical sample cells.

Different $\chi^{(3)}_{\text{sample}}$ components were measured using pulses of different polarizations. Zero-order halfwave plates, $\lambda/2$, and polarizers, P, were used to set the polarizations of pump 1, probe, and signal pulses (Scheme 1). When all beams had vertical polarization (further called *yyyy* polarization), component $\chi^{(3)}_{yyyy}$ was measured. For some experiments probe and signal beams were polarized horizontally (*xyyx* polarization; the first index denotes the signal polarization, and the last index, probe polarization) and component $\chi^{(3)}_{xyyx}$ was measured.

Results

Monomer and Polymer Synthesis. 3-Bromo-4-methoxyphenol (**1a**) was prepared according to a literature procedure.[13] **2a** was prepared from 3-bromo-4-methoxyphenol and the diazonium salt of 4-bromoaniline analogous to the procedure described previously by Schäfer and co-workers.[14] We recognized from previous work in the field that to create processable polymeric materials, we would need to have some substitution on the polymer backbone.[15] In addition, for future and potential applications we sought an unsymmetrical substitution pattern. With these considerations in hand we prepared monomers **3**, **5**, and **6** as outlined in Scheme 2.

The phenolic hydroxy group of substituted azobenzenes **2a** and **2b** was easily alkylated with 1-iodohexane to afford **3a** or alternatively protected as the *tert*-butyldimethylsilyl (TBDMS) ether. Palladium-catalyzed ethynylation[16] of the resulting dibromoazobenzene **3a** with (trimethylsilyl)acetylene followed by cleavage of the TMS group produced the diethynyl monomer **5a** in 81% isolated yield.

Polymer **7a** synthesized by cross coupling of **3a** and **5a** (Scheme 3) is soluble in common organic solvents, such as CH_2Cl_2, $CHCl_3$, and THF. The polymer was characterized by proton NMR spectroscopy and SEC analysis (Figure 1).

Polymer **7a** obtained in this synthetic route had much higher molecular weight (M_n = 18 400) than that made by an alternative cross-coupling reaction between **3a** and bis(tribu-

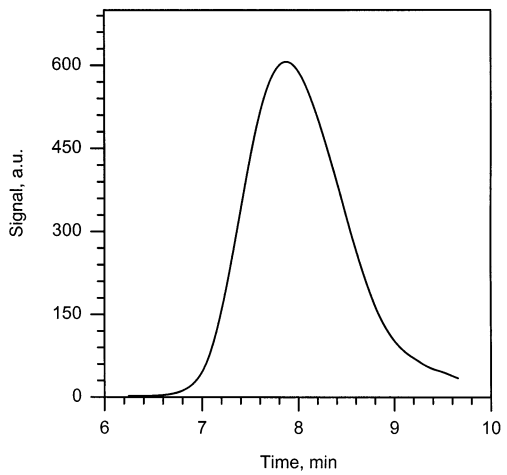

Figure 1. Size exclusion chromatogram of polymer **7a** (M_n = 18 400; polydispersity = 2.76). The molecular weight was measured relative to polystyrene standards.

SCHEME 3

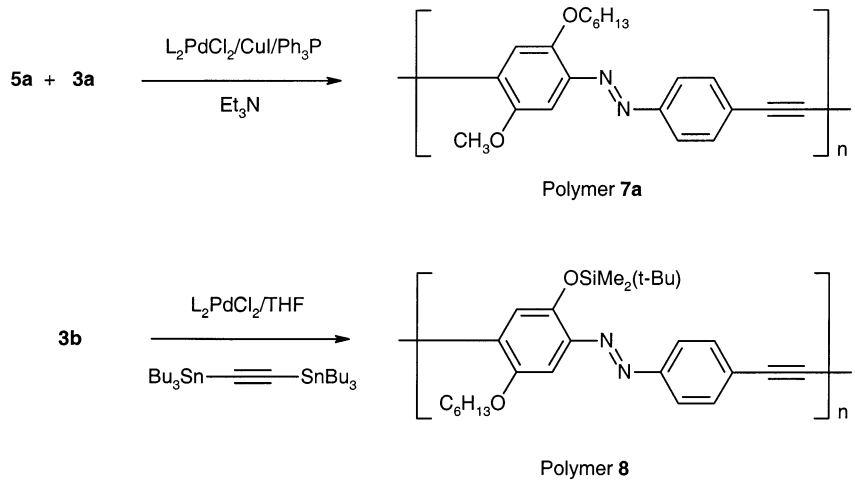

TABLE 2: Linear and Nonlinear Optical Characteristics of 3a and 7a in THF Solution

	abs max, nm	extinction coeff, L mol^{-1} cm^{-1}	fwhm,[a] cm^{-1}	Re γ,[b] $\times 10^{-49}$ m^5 V^{-2}	Im γ,[b] $\times 10^{-49}$ m^5 V^{-2}	$\lvert\gamma\rvert/\gamma_{THF}$ [c]	τ,[d] ps
3a	327	1.2×10^4	4775 ± 50	$\lvert 5.9 \pm 1.5\rvert$[e]		98	0.1
	399	9.0×10^3	4030 ± 35				
7a	383	1.4×10^4	7755 ± 280	$-(4300 \pm 300)$	1700 ± 300	7.7×10^4	0.1
	486	2.4×10^4	3200 ± 65				1.7 ± 0.3

[a] Estimated by fitting absorption bands to Gaussian functions. [b] Obtained by fitting concentration dependence data (Figure 6) to eq 6 and assuming $\chi^{(3)}_{THF} = 0.72 \times 10^{-22}$ m^2 V^{-2} (1×10^{-14} esu).[11,17] [c] **3a** and **7a** second hyperpolarizabilities were calculated as $\lvert\gamma\rvert = ((\mathrm{Re}\ \gamma)^2 + (\mathrm{Im}\ \gamma)^2)^{1/2}$; the THF second hyperpolarizability was assumed $\gamma_{THF} = 0.06 \times 10^{-49}$ m^5 V^{-2} (4.3×10^{-37} esu). [d] Response times were determined by fitting DFWM kinetics to one (for **3a**) and two (for **7a**) exponential functions, $I_{signal} = A_1 \exp(-t/\tau_1) + A_2 \exp(-t/\tau_2)$, where A_i is the amplitude of component i. [e] γ_{3a} sign could not be determined.

tylstannyl)acetylene ($M_n = 3100$). Polymerization of monomer **3b** with the bis(tributylstannyl)acetylene employing the palladium-catalyzed Stille coupling reaction produced polymer **8**. The incorporation of the silyl-protecting group provides an opportunity for future manipulation of the polymer backbone. Polymer **8** is also quite soluble in common organic solvents.

Absorption Spectra. Monomer **3a** and polymer **7a** electronic absorption spectra in THF solution are shown in Figure 2.

3a absorption maxima are at 327 nm (extinction coefficient $\epsilon_{327} = 1.2 \times 10^4$ L mol^{-1} cm^{-1}) and 399 nm ($\epsilon_{399} = 9.0 \times 10^3$ L mol^{-1} cm^{-1}); these strong absorption bands are attributed to $\pi-\pi^*$ transitions. The **7a** absorption spectrum is different from the **3a** spectrum. For **7a**, extinction coefficients are higher, absorption bands are broadened, and the maxima are shifted to 383 nm ($\epsilon_{383} = 1.4 \times 10^4$ L mol^{-1} cm^{-1}) and 486 nm ($\epsilon_{486} = 2.4 \times 10^4$ L mol^{-1} cm^{-1}). These features show that electronic coupling between the monomer units is strong, as is expected for the conjugated polymer **7a**. To estimate absorption band broadening for **7a**, both bands were fitted with the Gaussian functions. The fitting results are summarized in Table 2.

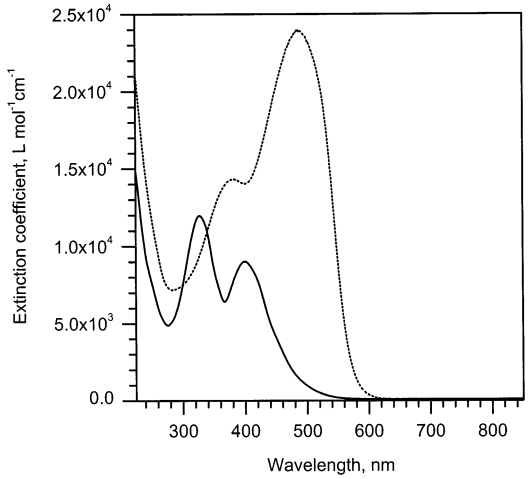

Figure 2. Electronic absorption spectra and linear extinction coefficients for **3a** (—) and **7a** (···) in THF solutions.

No aggregation or other concentration-dependent effects were observed in the absorption spectra up to the highest sample concentrations used in the experiments, 40 mmol for **3a** and 15 mmol for **7a**. Absorption spectra were periodically checked during and after the experiments. Because trans and cis isomers for azobenzenes[18,19] and related azo chromophores (such as Disperse Red dye, DR1)[20] have different electronic absorption spectra, the absence of spectral changes indicates that the azo chromophores did not undergo irreversible photoisomerization to the *Z*-isomer under the experimental conditions.

Intensity Dependence. Figure 3A,B shows DFWM signal intensity dependence for **3a** (concentration 13 mmol) and **7a** (concentration 6 mmol) solutions in THF; these signals are compared to the neat THF reference signal. Because pump1, pump2, and probe pulses are derived from a single laser pulse, the cubic intensity dependence is expected and is observed (but only at lower excitation intensity for **7a**). The data were analyzed by the nonlinear least-squares fitting of the signal, I_{sample}, to the expression $I_{sample} = mI_{excitation}{}^n$. Fitted exponents are $n = 2.99 \pm 0.03$ for neat THF, $n = 2.97 \pm 0.03$ for **3a** solution, and $n = 3.10 \pm 0.10$ for **7a** solution. For **7a**, only intensities $0.06I_{max} < I_{excitation} < 0.25I_{max}$ were included in the fit.

At high excitation intensity ($I_{excitation} > 0.30I_{max}$) the **7a** signal saturates and deviates from a simple power law (Figure 3); no such saturation is observed for **3a** at the same concentration and excitation intensity. Different processes can give rise to **7a**

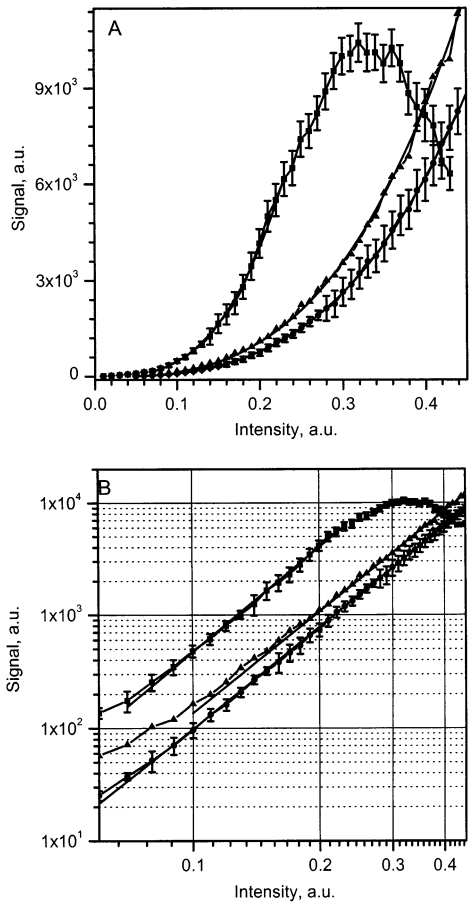

Figure 3. *yyyy* polarization DFWM signal dependence on the excitation intensity shown in linear scale (A) and log−log scale (B): (■) **7a** at 6 mmol concentration; (▲) **3a** at 13 mmol concentration; (●) neat THF. The excitation intensity is normalized in this graph; peak intensities of pump and probe pulses when intensity = 1 are given in Table 1. Data were fitted to the cubic power law as explained in the text; fit results are shown as solid lines.

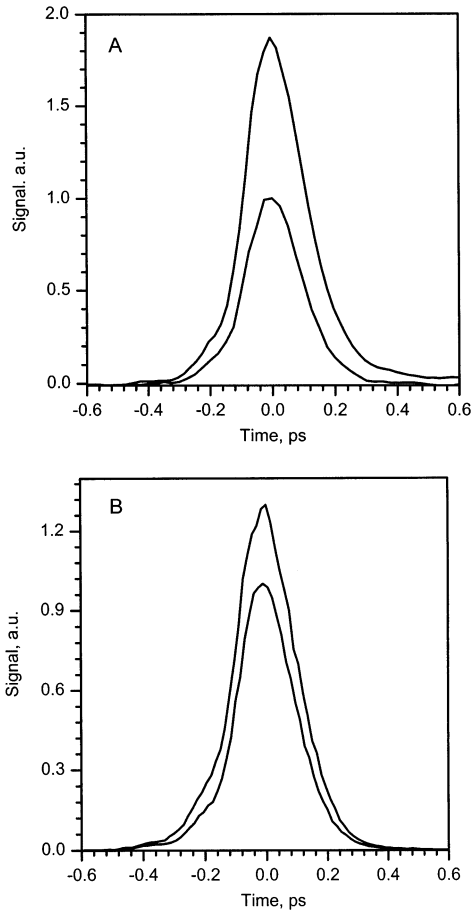

Figure 4. *yyyy* polarization DFWM kinetics measured at $I = 0.2I_{max}$ excitation: (A) kinetics for **7a** (4 mmol solution in THF); (B) kinetics for **3a** (20 mmol solution in THF). In both graphs smaller amplitude kinetics were measured for the neat THF reference.

signal saturation: (1) The real component of **7a** second hyperpolarizability, Re $\gamma^{(3)}$, is negative (see below), which leads to the laser beam defocusing at high intensities and can contribute to the apparent signal saturation. (2) Two-photon absorption (TPA) can also cause deviations from the cubic intensity dependence.[21] The azo chromophore TPA spectrum is similar to the ground-state spectrum;[22] support for TPA is also found in kinetics data (see below). By assuming that the signal deviates from the expected $I_{signal} \propto I_{excitation}^3$ only due to TPA, the upper limit of the two-photon absorption coefficient, α_2, can be estimated by fitting the **7a** intensity dependence to eq 2. This analysis yields $(\alpha_2 l) = 2.5 \times 10^{-5}$ m^2 G W^{-1}; when $l = 1$ mm (l is optical path in the sample cell) $\alpha_2 = 0.025$ m G W^{-1}. However, the beam overlap region (transient grating in the sample) is smaller; for the beam geometry used in experiments the transient grating thickness was $l_{TG} = 60$ μm. This l_{TG} value yields $\alpha_2 = 0.42$ m G W^{-1}. The estimated TPA coefficient can be compared to $\alpha_2 = 1.7 \times 10^{-3}$ m G W^{-1} for a DR1/PMMA side chain polymer (determined by Z-scan with 150 fs pulses at 820 nm, PMMA is poly(methyl methacrylate)).[23] *Therefore, polymer **7a** has a much higher nonlinear absorption coefficient than the DR1 dye and exhibits optical limiting at 780 nm.* Further studies of optical limiting by Z-scan techniques could be used to more accurately determine two-photon absorption coefficient.

Nonlinear Kinetics. DFWM kinetics were measured at $I_{excitation} = 0.2I_{max}$ (intensity = 0.2 in Figure 3), where the **7a** signal follows the cubic power law. **3a** and **7a** *yyyy* polarization DFWM kinetics show a pulse-width limited response (fwhm = 200 ± 20 fs, Figure 4). In addition to the major $\tau_1 \approx 100$ fs component, the **7a** DFWM signal also has a slower-decaying component with about 50−100 times smaller amplitude (see below). Instantaneous DFWM signals are characteristic of electronic nonlinearity. In contrast, orientational or isomerization-related nonlinearities would be observed on the slower time scales.

Additional information about the nonlinear mechanism can be obtained by comparing *yyyy* and *xyyx* polarization kinetics. In solution (isotropic medium) tensor $\chi^{(3)}_{sample}$ has only three independent components, and $\chi^{(3)}_{yyyy} = \chi^{(3)}_{xyyx} + \chi^{(3)}_{yxyx} + \chi^{(3)}_{yyxx}$.[24] When the experimental wavelength is far from the one-photon resonance, Kleinman symmetry also applies and $\chi^{(3)}_{xyyx} = \chi^{(3)}_{yxyx} = \chi^{(3)}_{yyxx}$. Therefore, for electronic nonlinearity far from resonance the expected $\chi^{(3)}_{sample}$ component ratio is $\chi^{(3)}_{yyyy}/\chi^{(3)}_{xyyx} = 3$.

Figure 5 shows **7a** *yyyy* polarization (A) and *xyyx* polarization (B) DFWM kinetics measured at $I_{excitation} = 0.3I_{max}$ (intensity = 0.3 in Figure 3). The ratio of the kinetic amplitudes is $I_{yyyy}/I_{xyyx} = [\chi^{(3)}_{yyyy}/\chi^{(3)}_{xyyx}]^2 = 8.60 \pm 0.25$, or $\chi^{(3)}_{yyyy}/\chi^{(3)}_{xyyx} = 2.90 \pm 0.15$. Therefore, both instantaneous response on $\tau_1 = 100$ fs time scale and $\chi^{(3)}_{yyyy}/\chi^{(3)}_{xyyx}$ value support DFWM signal assignment to the electronic nonlinearity.

Comparison of **7a** *yyyy* and *xyyx* polarization kinetics in Figure 5 also reveals that only *yyyy* polarization kinetics has a small picosecond component. As shown in the inset of Figure 5A, the data measured on the longer time scale can be fitted

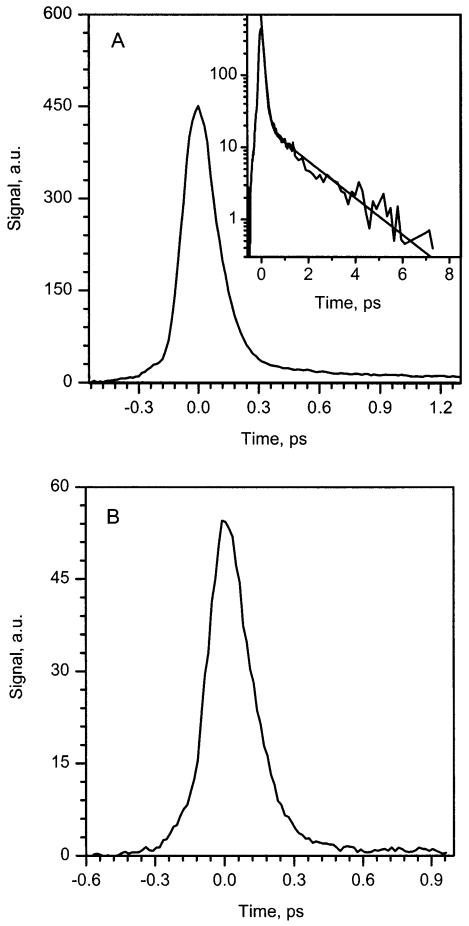

Figure 5. **7a** *yyyy* (A) and *xyyx* (B) polarization DFWM kinetics. Data were measured in 10 mmol solutions with $I = 0.3I_{max}$ excitation. The inset in A shows longer time kinetics on a log-linear scale and a two exponential fit with $\tau_1 = 100$ fs (0.97 amplitude) and $\tau_2 = 1.7 \pm 0.3$ ps (0.03 amplitude) lifetime components.

with $\tau_1 = 100$ fs (0.97 amplitude) and $\tau_2 = 1.7 \pm 0.3$ ps (0.03 amplitude) lifetimes. *xyyx* polarization DFWM measurements do not probe populations of the excited states, whereas *yyyy* polarization measurements reflect thermalization dynamics originating from the molecular excited states. Because the $\tau_2 = 1.7$ ps component is observed only in the *yyyy* configuration and its amplitude increases at higher excitation intensity (amplitude is 0.03 at $I_{excitation} = 0.3I_{max}$ and <0.02 at $I_{excitation} = 0.2I_{max}$, Figure 4), the 1.7 ps component is assigned to **7a** excited-state dynamics. Two-photon absorption leading to **7a** excited-state formation was also inferred from the DFWM signal saturation in the intensity dependence (Figure 3). Within the signal-to-noise ratio for the experiment, the τ_2 lifetime was the same in kinetics measured with $I_{excitation} = 0.3I_{max}$ and $I_{excitation} = 0.2I_{max}$.

Second Hyperpolarizability from Concentration Dependence Data. Nonlinear susceptibility concentration dependence data (Figure 6) were obtained by verifying the cubic intensity dependence, $I_{sample} \propto I_{excitation}^{3.0\pm0.1}$, at each sample concentration and then measuring kinetics with $I_{excitation} = 0.2I_{max}$. Solution and neat THF kinetics amplitudes at $t = 0$ were used to calculate the susceptibility ratio according to eq 3; $\alpha = 0$ was assumed. The results show that polymer **7a** solution susceptibility *decreases* at low polymer concentration, reaches a minimum at about 1.3 mmol and becomes larger than the solvent susceptibility at about 3 mmol.

Although a DFWM measurement at a single concentration does not yield the sign of third-order nonlinearity (because

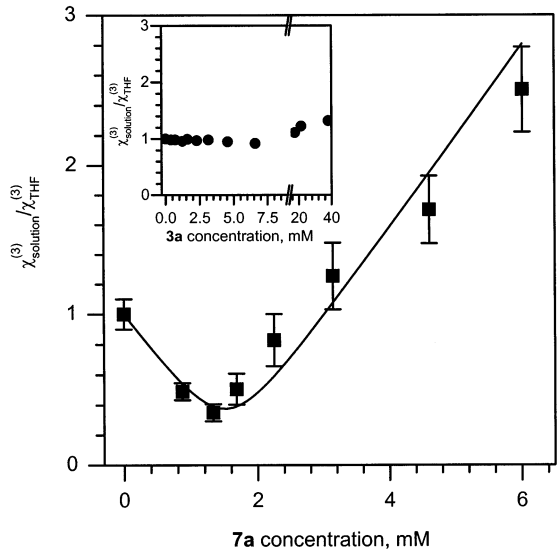

Figure 6. Concentration dependence for **7a** (■) and **3a** (●, inset) third-order susceptibilities in THF solution. The data were obtained with $I = 0.2I_{max}$ excitation in *yyyy* polarization measurements. The solid line shows a nonlinear least-squares fit of **7a** data to eq 6. Second hyperpolarizability values are Re $\gamma_{7a} = -(4.3 \pm 0.3) \times 10^{-46}$ m^5 V^{-2} and Im $\gamma_{7a} = (1.7 \pm 0.3) \times 10^{-46}$ m^5 V^{-2}.

$I_{sample} \propto |\chi^{(3)}_{sample}|^2$ − eq 2), the concentration dependence study allows us to determine the sign. Macroscopic $\chi^{(3)}_{sample}$ is related to solute and solvent second hyperpolarizabilities, γ_{solute} and $\gamma_{solvent}$, as[11]

$$\chi^{(3)}_{sample} = f^4(N_{solute}\gamma_{solute} + N_{solvent}\gamma_{solvent}) \quad (4)$$

where f is the Lorentz local field factor (for isotropic liquid $f = (n^2 + 2)/3$,[24] and N is a molecular number density (number of molecules per cubic meter). γ_{solute} can have real and imaginary components: $\gamma_{solute} = \text{Re}\,\gamma_{solute} + \text{i Im}\,\gamma_{solute}$, i is an imaginary unit, $\text{i}^2 = -1$. Re γ_{solute} is related to nonlinear refraction index changes in the sample, Im γ_{solute} is related to the two-photon absorption. For low concentration solutions $\chi^{(3)}_{solvent} \approx f^4 N_{solvent}\gamma_{solvent}$ and eq 4 can be written as

$$\chi^{(3)}_{sample} = f^4 N_{solute}\gamma_{solute} + \chi^{(3)}_{solvent} \quad (5)$$

The absolute value of susceptibility, $|\chi^{(3)}_{sample}|$, is[11]

$$|\chi^{(3)}_{sample}| = (|f^4 N_{solute}\,\text{Re}\,\gamma_{solute} + \chi^{(3)}_{solvent}|^2 + |f^4 N_{solute}\,\text{Im}\,\gamma_{solute}|^2)^{1/2} \quad (6)$$

Third-order susceptibility is measured in m^2 V^{-2}; values reported in these SI units are related to commonly used esu units as $\chi^{(3)}(\text{esu}) = 9 \times 10^8/4\pi\chi^{(3)}(\text{SI})$.[24] Second hyperpolarizability is measured in m^5 V^{-2} (SI units) and can be expressed in esu units as $\gamma(\text{esu}) = 9 \times 10^{14}/4\pi\gamma(\text{SI})$.[24] We have adapted the suggested THF third-order susceptibility value, $\chi^{(3)}_{THF} = 1.4 \times 10^{-22}$ m^2 V^{-2} (1×10^{-14} esu).[11] A similar value ($\chi^{(3)}_{THF} = (1.2 \pm 0.3) \times 10^{-14}$ esu) was recently reported in optical Kerr effect studies at 800 nm with 100 fs pulses.[17]

According to eq 6, the initial $\chi^{(3)}_{solution}/\chi^{(3)}_{THF}$ decrease in Figure 6 clearly demonstrates that Re $\gamma_{7a} < 0$ (because solvent Re $\gamma_{THF} > 0$). Because the solution susceptibility does not reach zero in Figure 6, Im $\gamma_{7a} \neq 0$. The second hyperpolarizability values were determined by nonlinear least-squares fitting of the data to eq 6, yielding Re $\gamma_{7a} = -(4.3 \pm 0.3) \times 10^{-46}$ m^5 V^{-2}

and $|\mathrm{Im}\ \gamma_{7a}| = (1.7 \pm 0.3) \times 10^{-47}$ m^5 V^{-2} (Table 2). The negative Re γ_{7a} value is interesting, because materials with Re $\gamma < 0$ are relatively rare, but potentially important in optical device applications. In materials with Re $\gamma < 0$ the laser beam is defocused due to the self-action, and this defocusing protects the organic material from damage.

3a concentration dependence data were also collected. Because of the smaller γ_{3a} value, it was not possible to determine susceptibility changes at lower **3a** concentrations, and therefore, Re γ_{3a} and Im γ_{3a} values could not be determined. At the highest concentration (38 mmol) the **3a** solution signal had an amplitude 1.4 times larger than that of the solvent (Figure 6 and kinetics in Figure 4). From these data, it is possible to estimate the **3a** second hyperpolarizability $|\gamma_{3a}| = (5.9 \pm 1.5) \times 10^{-49}$ m^5 V^{-2}. Therefore, the second hyperpolarizability (calculated per repeat unit) is about 780 times larger for polymer **7a** as compared to monomer **3a**. It was previously found that Re $\gamma < 0$ for azo chromophores similar to **3a**,[7,25,26] and thus it is likely that γ_{3a} is also negative.

Discussion

Mechanism of Third-Order Nonlinearity. On the basis of the instantaneous time response, $\tau_1 = 100$ fs, and third-order susceptibility tensor component ratio, $\chi^{(3)}_{yyyy}/\chi^{(3)}_{xyyx} = 3$, the nonlinearity is electronic. A concentration dependence study was used to determine second hyperpolarizability of monomer **3a** and polymer **7a** (Figure 6); values are summarized in Table 2. Next, we consider quantum chemical description of second hyperpolarizability using a three-state model:[10,21,25,27−29]

$$\gamma \propto \frac{M_{01}{}^2 \Delta\mu^2}{(\omega_{01} - \omega - i\Gamma_{01})^3} - \frac{M_{01}{}^4}{(\omega_{01} - \omega - i\Gamma_{01})^3} + \frac{M_{01}{}^2 M_{12}{}^2}{(\omega_{01} - \omega - i\Gamma_{01})^2(\omega_{02} - 2\omega - i\Gamma_{02})} \quad (7)$$

where M_{01} is the transition dipole moment to the one-photon state, M_{12} is the transition dipole moment between the one-photon and two-photon states, ω_{01} and ω_{02} are frequencies for transitions between the excited (one-photon and two-photon) states and the ground state, Γ_{01} and Γ_{02} are dephasing parameters that account for the linewidths. The first term in eq 7 is related to the dipole moment difference between the first excited and the ground states ($\Delta\mu = \mu_{11} - \mu_{00}$). This term is positive, and is only available in noncentrosymmetric molecules. The contributions of the second and third terms in eq 7 determine the magnitude and the sign of γ for many molecules.[10] Using the model of eq 7, large negative γ_{7a} can be related to:

(1) Nonlinearity due to one-photon state is represented by the second term of eq 7. Theoretical and experimental studies of donor and acceptor substituted polyenes revealed that the second term will be dominant and γ will have a large negative value when the bond-length alteration in the molecule is minimal.[27] Structural rigidity was also proposed to determine large negative γ values, for example, in squarylium dyes.[28] Negative γ in metal-substituted azo derivatives was recently assigned to this mechanism.[25] Polymer **7a** does have necessary electronic symmetry and structural rigidity − strong electronic coupling between the monomer units is evident from the absorption spectrum (Figure 2), and the alkynyl linkages in a polymer backbone provide for structural rigidity. Therefore, nonlinearity due to the one-photon term is likely to be important for **7a**.

(2) Contribution from the two-photon state (last term of eq 7) can also determine the negative sign of γ_{7a}. When the energy of the two-photon state, E_{02} ($E_{02} = \hbar\omega_{02}$), is below the two-photon resonance, the two-photon term will have a negative sign (i.e., this term will be negative if the two-photon-state energy E_{02} is less than 25 640 cm^{-1}, because 780 nm = 12 820 cm^{-1}). The elusive two-photon state is largely unknown, and its existence is usually postulated or inferred indirectly, such as, for example, in conjugated porphyrin oligomers.[21,30] In conjugated polymers and oligomers two-photon state is either a charge transfer or a singlet biexciton state.[9,10] Formation of such a state was directly observed in kinetics (Figure 5A), but the energy of this state is not known. Frequency dispersion data for γ_{7a} are required for definite assignment, because at different experimental wavelengths nonlinearity due to the two-photon state would change the sign.

7a Excited-State Lifetime. In addition to pulse-width limited electronic nonlinearity, a small 1.7 ps lifetime component was observed in **7a** DFWM kinetics. Within the signal-to-noise ratio for the experiment, this component is only observed in *yyyy* polarization experiments and is not present in **3a** solution kinetics at either polarization. *yyyy* polarization DFWM kinetics reflects the concentration of molecules in the excited state, and the 1.7 ps component is attributed to the **7a** excited state formed by two-photon excitation. When the excited state decays with the first-order rate constant, k, the DFWM signal is time dependent as $I_{\mathrm{sample}} = I_{0,\mathrm{sample}} \exp(-2kt)$, where $I_{0,\mathrm{sample}}$ is the signal amplitude at $t = 0$.[8,11] Therefore (provided that observed kinetics is first-order), **7a** excited-state lifetime, τ_{ES}, can be estimated as $\tau_{ES} = 1.7 \times 2 = 3.4$ ps, or $k = (3.4\ \mathrm{ps})^{-1} = 2.9 \times 10^{11}$ s^{-1}. Similar excited-state kinetics components with lifetimes in the several picosecond range have been reported for several azobenzene derivatives.[31] These transient absorption picosecond dynamics were attributed to trans → cis[18,32] and cis → trans[19] isomerization. Because of the difference between substituted azobenzenes and polymer **7a**, assignment of the observed $k = 2.9 \times 10^{11}$ s^{-1} rate constant process to the isomerization, intersystem crossing, or biexciton dynamics must await detailed transient absorption studies. The small amplitude of the $\tau_2 = 1.7$ ps component does not preclude analysis of femtosecond electronic nonlinearity, which is dominant (>0.98 signal amplitude at excitation intensity used in concentration dependence experiments).

Comparison with Third-Order Nonlinear Azo Side-Chain Polymers. To our knowledge, this is the first report of the nonlinear optical properties of a conjugated polymer incorporating an azo linkage in the polymer backbone. Earlier studies examined third-order nonlinearities in azo dyes and in polymers with the side chains containing azo groups.[7,20,22,23,26,33−37] Perhaps the most commonly studied azo chromophore is DR1 dye:[20,22,23,26,33,34]

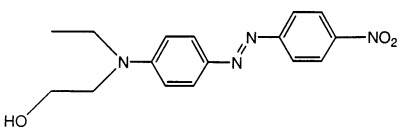

The second hyperpolarizability of DR1 is similar to that of **3a**. For example, in PMMA/DR1 thin films Re $\chi^{(3)}_{\mathrm{DR1}} = -6.6 \times 10^{-18}$ m^2 V^{-2} were reported (Z-scan studies with 20 ps pulses at 610 nm).[26] The second hyperpolarizability can be estimated as $|\mathrm{Re}\ \gamma_{\mathrm{DR1}}| = |\mathrm{Re}\ \chi^{(3)}_{\mathrm{DR1}}/(Nf^4)| = 2.3 \times 10^{-49}$ m^5 V^{-2} (because $N = 5.6 \times 10^{26}$ m^{-3} and $f = 5.0$ ($n = 1.58$)).[26] This Re γ_{DR1} value is about half the value of $|\gamma_{3a}| = 5.9 \times 10^{-49}$ m^5 V^{-2} (Table 2).

In contrast to conjugated polymer **7a**, attaching side-chain azo chromophores to the polymer backbone does not change γ significantly.[7,33] For example, $\chi^{(3)} = 13.2 \times 10^{-21}$ m^2 V^{-2} (20 mmol solution in CH_2Cl_2, Z scan measurements at 1064 nm with 50 ps pulses) *decreased* to $\chi^{(3)} = 10.5 \times 10^{-21}$ m^2 V^{-2} (same chromophore concentration) when DR1 was covalently attached to the maleic anhydride and octadecene copolymer backbone.[33] Because of the weak electronic interaction, the two-photon absorption coefficient also did not change in the azo side-chain polymer,[33] whereas we observed a large increase in the two-photon absorption coefficient for polymer **7a** (see Results).

Very large thermal[35,36] and orientational nonlinearies (including nonlinearity due to photoisomerization of the azo linkage)[37] have also been reported for azo chromophores, but they do not provide the femtosecond/picosecond response times required for optical switching applications.[7]

In summary, we have synthesized new conjugated organic polymers containing azo groups and alkynyl linkages in the polymer backbone and have characterized third-order nonlinear optical properties in THF solution. The polymer **7a** second hyperpolarizability is $\gamma_{7a} = (4.6 \pm 0.5) \times 10^{-46}$ m^5 V^{-2}. The γ_{7a} value per polymer repeat unit is about 780 times larger than γ_{3a} for the corresponding monomer **3a**. Significant γ enhancement is attributed to the conjugation in the polymer backbone and rigid coupling between the monomer units, as well as contribution from a two-photon state. Large electronic nonlinearity has a negative sign and a femtosecond response ($\tau_1 =$ 100 fs), making it interesting for further studies and optical device applications.[7]

Acknowledgment. We are grateful to the Office of Naval Research for partial funding of this research. M.P. thanks the Alexander von Humboldt Foundation for a Feodor Lynen Research Fellowship. D.K. acknowledges generous start-up support from VCU and Jeffress Memorial Trust for partial support of this research.

Supporting Information Available: Synthesis of compounds **1**−**8** and characterization by ^{1}H and ^{13}C NMR, elemental analysis, and SEC. This material is available free of charge via the Internet at http://pubs.acs.org.

References and Notes

(1) *Handbook of Conducting Polymers*; Skotheim, T. J., Ed.; Dekker: New York, 1986 (see also references therein).

(2) Zhou, Q.; Swager, T. M. *J. Am. Chem. Soc.* **1995**, *117*, 12593 and references therein.

(3) Lessard, R. A.; Couture, J. J. A. *Mol. Cryst. Liq. Cryst.* **1990**, *183*, 451 and references therein.

(4) Kim, D. Y.; Li, L.; Jiang, X. L.; Shrivshanker, V.; Kumar, J.; Tripathy, S. K. *Macromolecules* **1995**, *28*, 8835.

(5) Rochon, P.; Batalla, E.; Natansohn, A. *Appl. Phys. Lett.* **1995**, *66*, 136.

(6) Tripathy, S. K.; Kim, D. Y.; Lee, T. S.; Jiang, X. L.; Li, L.; Kumar, J. *Polym. Prepr. (Am. Chem. Soc., Div. Polym. Chem.)* **1996**, *37* (1), 123.

(7) Brzozowski, L.; Sargent, E. H. *J. Mater. Sci.-Mater.* **2001**, *12*, 483.

(8) Eichler, H. J.; Günter, P.; Pohl, D. W. *Laser-Induced Dynamic Gratings*; Springer-Verlag: Berlin, 1986.

(9) Kuebler, S. M.; Denning, R. G.; Anderson, H. L. *J. Am. Chem. Soc.* **2000**, *122*, 339.

(10) Gubler, U.; Bosshard, C. Molecular Design for Third-Order Nonlinear Optics. In *Polymers in Photonics Applications I*; Lee, K.-S., Ed.; Springer: Berlin, 2002; p 123.

(11) Prasad, P. N.; Williams, D. J. *Introduction to Nonlinear Optical Effects in Molecules and Polymers*; John Wiley & Sons: New York, 1991.

(12) *CRC Handbook of Chemistry and Physics*, 77th ed.; Lide, D. R., Ed.; CRC Press: Boca Raton, FL, 1996.

(13) Giles, R. G.; Hughes, A. B.; Sargent, M. V. *J. Chem. Soc., Perkin Trans. 1* **1991**, *6*, 1581.

(14) Pardo, M.; Joos, K.; Schäfer, W. *Liebigs Ann. Chem.* **1982**, 99.

(15) Maruyama, T.; Kubota, K.; Yamamoto, T. *Macromolecules* **1993**, *26*, 4055 and references therein.

(16) Neenan, T. X.; Whitesides, G. M. *J. Org. Chem.* **1988**, *53*, 2489.

(17) Slepkov, A. D.; Hegmann, F. A.; Zhao, Y. M.; Tykwinski, R. R.; Kamada, K. *J. Chem. Phys.* **2002**, *116*, 3834.

(18) Lednev, I. K.; Ye, T. Q.; Abbott, L. C.; Hester, R. E.; Moore, J. N. *J. Phys. Chem. A* **1998**, *102*, 9161.

(19) Nagele, T.; Hoche, R.; Zinth, W.; Wachtveitl, J. *Chem. Phys. Lett.* **1997**, *272*, 489.

(20) Loucif-Saibi, R.; Nakatani, K.; Delaire, J. A.; Dumont, M.; Sekkat, Z. *Chem. Mater.* **1993**, *5*, 229.

(21) Thorne, J. R. G.; Kuebler, S. M.; Denning, R. G.; Blake, I. M.; Taylor, P. N.; Anderson, H. L. *Chem. Phys.* **1999**, *248*, 181.

(22) Delysse, S.; Raimond, P.; Nunzi, J. M. *Chem. Phys.* **1997**, *219*, 341.

(23) Yamakawa, S.; Hamashima, K.; Kinoshita, T.; Sasaki, K. *Appl. Phys. Lett.* **1998**, *72*, 1562.

(24) Butcher, P. N.; Cotter, D. *The Elements of Nonlinear Optics*; Cambridge University Press: Cambridge, U.K., 1990.

(25) Wu, S. J.; Qian, W.; Xia, Z. J.; Zou, Y. G.; Wang, S. Q.; Shen, S. Y.; Xu, H. J. *Chem. Phys. Lett.* **2000**, *330*, 535.

(26) Rangel-Rojo, R.; Yamada, S.; Matsuda, H.; Yankelevich, D. *Appl. Phys. Lett.* **1998**, *72*, 1021.

(27) Meyers, F.; Marder, S. R.; Pierce, B. M.; Brédas, J. L. *J. Am. Chem. Soc.* **1994**, *116*, 10703.

(28) Dirk, C. W.; Herndon, W. C.; Cervanteslee, F.; Selnau, H.; Martinez, S.; Kalamegham, P.; Tan, A.; Campos, G.; Velez, M.; Zyss, J.; Ledoux, I.; Cheng, L. T. *J. Am. Chem. Soc.* **1995**, *117*, 2214.

(29) Brédas, J. L.; Adant, C.; Tackx, P.; Persoons, A.; Pierce, B. M. *Chem. Rev.* **1994**, *94*, 243.

(30) Terazima, M.; Shimizu, H.; Osuka, A. *J. Appl. Phys.* **1997**, *81*, 2946.

(31) Tamai, N.; Miyasaka, H. *Chem. Rev.* **2000**, *100*, 1875.

(32) Hirose, Y.; Yui, H.; Sawada, T. *J. Phys. Chem. A* **2002**, *106*, 3067.

(33) Cherioux, F.; Audebert, P.; Maillotte, H.; Grossard, L.; Hernandez, F. E.; Lacourt, A. *Chem. Mater.* **1997**, *9*, 2921.

(34) Churikov, V. M.; Hsu, C. C. *J. Opt. Soc. Am. B* **2001**, *18*, 1722.

(35) Wang, Y. G.; Zhao, J. A.; Si, J. H.; Ye, P. X.; Fu, X. F.; Qiu, L.; Shen, Y. Q. *J. Chem. Phys.* **1995**, *103*, 5357.

(36) Fei, H. S.; Wei, Z. Q.; Yang, Q. G.; Che, Y. L.; Shen, Y. Q.; Fu, X. F.; Qiu, L. *Opt. Lett.* **1995**, *20*, 1518.

(37) Dong, F.; Koudoumas, E.; Couris, S.; Shen, Y. Q.; Qiu, L.; Fu, X. F. *J. Appl. Phys.* **1997**, *81*, 7073.